AGU PUBLICATIONS

Water Resources Research

RESEARCH ARTICLE
10.1002/2013WR014818

Special Section:
Patterns in Soil-Vegetation-Atmosphere Systems: Monitoring, Modelling and Data Assimilation

Optimization of canopy conductance models from concurrent measurements of sap flow and stem water potential on Drooping Sheoak in South Australia

Hailong Wang[1,2], Huade Guan[1,2], Zijuan Deng[1,2], and Craig T. Simmons[1,2]

[1]School of the Environment, Flinders University, Adelaide, South Australia, Australia, [2]National Centre for Groundwater Research and Training, Flinders University, Adelaide, South Australia, Australia

Key Points:
- We selected the best canopy conductance model for a native species in Adelaide
- Selection of proper stress functions is important for conductance modeling
- Temperature effect is different from other studies and nonignorable

Correspondence to:
H. Wang,
hailong.wang@flinders.edu.au

Citation:
Wang, H., H. Guan, Z. Deng, and C. T. Simmons (2014), Optimization of canopy conductance models from concurrent measurements of sap flow and stem water potential on Drooping Sheoak in South Australia, *Water Resour. Res.*, *50*, 6154–6167, doi:10.1002/2013WR014818.

Received 30 SEP 2013
Accepted 4 JUL 2014
Accepted article online 10 JUL 2014
Published online 29 JUL 2014

Abstract Canopy conductance (g_c) is a critical component in hydrological modeling for transpiration estimate. It is often formulated as functions of environmental variables. These functions are climate and vegetation specific. Thus, it is important to determine the appropriate functions in g_c models and corresponding parameter values for a specific environment. In this study, sap flow, stem water potential, and microclimatic variables were measured for three Drooping Sheoak (*Allocasuarina verticillata*) trees in year 2011, 2012, and 2014. Canopy conductance was calculated from the inversed Penman-Monteith (PM) equation, which was then used to examine 36 g_c models that comprise different response functions. Parameters were optimized using the DiffeRential Evolution Adaptive Metropolis (DREAM) model based on a training data set in 2012. Use of proper predawn stem water potential function, vapor pressure deficit function, and temperature function improves model performance significantly, while no pronounced difference is observed between models that differ in solar radiation functions. The best model gives a correlation coefficient of 0.97, and root-mean-square error of 0.0006 m/s in comparison to the PM-calculated g_c. The optimized temperature function shows different characteristics from its counterparts in other similar studies. This is likely due to strong interdependence between air temperature and vapor pressure deficit in the study area or Sheoak tree physiology. Supported by the measurements and optimization results, we suggest that the effects of air temperature and vapor pressure deficit on canopy conductance should be represented together.

1. Introduction

Vegetation plays an important role in land surface hydrological processes, and coordinates the land-atmosphere interactions in a wide range of spatial scales [*Dickinson*, 1987; *Avissar and Pielke*, 1989; *Chen et al*., 1996; *LeMone et al*., 2007]. It regulates water transport in the soil-plant-atmosphere continuum by means of stomata behavior [*Rao and Agarwal*, 1984; *Alfieri et al*., 2008]. Among approaches of quantifying this regulation, the "big leaf" model in the Penman-Monteith (PM) equation [*Monteith*, 1981] has been widely discussed and applied [*Leuning and Foster*, 1990; *Lu et al*., 2003]. The PM equation represents bulk stomata behavior as canopy resistance (r_c), and assumes that stomata and canopy resistance have the same influencing factors [*Lhomme et al*., 1998], including air temperature (T), vapor pressure deficit (D), solar radiation (R_s), CO_2 concentration, soil water content (θ), and leaf water potential (ψ_l) [*Jarvis*, 1976; *Tuzet et al*., 2003; *Damour et al*., 2010].

Response of canopy conductance to the influencing factors has been incorporated into land surface models for transpiration estimate, such as in *Noilhan and Planton* [1989]. Many studies constructed canopy conductance model following the Jarvis-Stewart approach [*Jarvis*, 1976; *Stewart*, 1988], which calculated canopy conductance from a maximum stomatal conductance by applying different stress functions related to influencing factors. For example, *Thorpe et al*. [1980] presented stomatal conductance of apple trees in terms of photon flux density and leaf to air vapor pressure gradient; *Ball et al*. [1987] and *Collatz et al*. [1991] linked stomatal conductance to CO_2 assimilation using a function of intercellular CO_2 concentration and leaf-level relative humidity; *White et al*. [1999] related canopy resistance to solar radiation, air temperature, and vapor pressure deficit for eucalyptus trees; *Lu et al*. [2003] modeled grapevine canopy conductance with solar radiation and vapor pressure deficit. More similar studies can be found in a recent review paper by *Damour et al*. [2010].

The gradient of water potentials in soil, stem, and leaf drives water transport in the soil-plant-atmosphere system [*Vandegehuchte et al*., 2014b]. Plant water potential is a sensitive indicator for vegetation water status [*Choné et al*., 2001; *Nortes et al*., 2005] and is constrained by stomata regulation of transpiration [*Meinzer et al*., 2008]. Leaf water potential has been discussed in stomata regulation of water transport in a few studies [*Jarvis*, 1976; *Comstock and Mencuccini*, 1998; *Macfarlane et al*., 2004; *Misson et al*., 2004]. Plant water potential is less favorable in vegetation water use and canopy conductance modeling, due to the difficulty in measuring leaf/stem water potential continuously. Many studies after *Jarvis* [1976] used soil water content [*Stewart*, 1988; *Gash et al*., 1989] instead of plant water potential. However, most soil water content measurements only cover shallow soil layers up to 2 m deep, commonly within 50 cm [*Whitley et al*., 2008]. Those measurements can reflect water availability to vegetation with shallow root systems; however, it is doubted that they can capture the whole picture of water uptake for vegetation with deep roots, because the "wet" zones in the soil are progressively deeper during soil drying cycles [*White et al*., 2003], and some vegetation can access groundwater storage in dry periods [*Murray et al*., 2003; *Eamus and Froend*, 2006]. In addition, storage of water in trees can also contribute to a certain proportion of the daily sap flux, especially when soil dries up [*Edwards and Jarvis*, 1982; *Tyree and Yang*, 1990; *Phillips et al*., 1996; *Meinzer et al*., 2004]. Predawn stem water potential (ψ_{pd}) can be taken as a good approximate of root-zone soil water condition [*Palmer et al*., 2010], because water potential is in equilibrium within the entire soil-plant continuum [*Richter*, 1997] at predawn. Recent technical advance allows monitoring stem water potential continuously [*Patankar et al*., 2013; *Yang et al*., 2013; *Vandegehuchte et al*., 2014b, 2014a], which makes it more feasible to investigate the relationship between vegetation water use and stem and root-zone water potential.

The stress of each influencing factor on canopy conductance is site specific and has been expressed differently among studies. Selection of response functions in many studies is somewhat arbitrary, without an explanation on why they, not others, were chosen. We hypothesize that selecting the appropriate functions will lead to better simulations of canopy conductance. The primary objective of this study is therefore to test this hypothesis by comparing simulation results from various response functions. The effect of temperature on canopy conductance is often neglected without quantitative evidence [*Mascart et al*., 1991; *Lhomme et al*., 1998]. Significance of the temperature effect is specifically examined in this study. Measurements of sap flow and stem water potential were conducted on Drooping Sheoak trees (*Allocasuarina verticillata*) in Adelaide, South Australia. This species is endemic to Australia, and widely distributed from Queensland to Tasmania and westward to South Australia. Its ability to develop extensive root systems in poor coastal soils (including sand dunes) makes it a valuable soil stabilizer. It is also valued for its provision of habitat for cockatoos [*Chapman and Paton*, 2007]. The areal extent of Drooping Sheoak has dramatically decreased in South Australia since the European Settlement [*Peeters et al*., 2006]. Although climate is known to cause Drooping Sheoak mortality [*Peeters et al.,* 2006], little specific research has been conducted on its water use in response to environmental variables.

2. Methodology

2.1. Site Description

The study site is near the campus of Flinders University (138°34′28″E, 35°01′49″S). Ground surface is covered by sparse trees with short shrubs and grass at substrate. Soil type is characterized as sandy mixed with gravel. This soil condition makes it difficult to bury soil moisture probes for water content measurement near the trees.

The site is in Mediterranean climate zone. Annual mean temperature is about 17°C, and annual rainfall is around 546 mm, most of which occurs in May-September [*Guan et al*., 2013]. Three Drooping Sheoak trees were selected for sap flow and stem water potential measurements in this study. Measurements were conducted in March-May 2011 (31 days) on tree 1 [*Yang et al*., 2013], January-April and October-December 2012 (150 days) on tree 2, and April-June 2014 (27 days) on tree 3.

2.2. Sap Flow and Stem Water Potential Measurements

Sap flow was monitored at 30 min intervals in the tree trunks at 1.3 m above ground using the compensation heat-pulse technique (HPV) [*Green and Clothier*, 1988] for tree 1 in 2011 and tree 2 in 2012, and heat ratio method (HRM) [*Burgess et al*., 2001] for tree 3 in 2014. For HPV method, three thermocouples are embedded inside each temperature probe at the depths of 5, 15, and 25 mm underneath the cambium.

One temperature probe was installed 10 mm above the heater and the other 5 mm below the heater. Two sets of such probes were installed in the south and north sides of tree trunks. For HRM method, two thermocouples are embedded at 12.5 and 27.5 mm underneath the cambium. Two temperature probes were symmetrically installed at 5 mm above and below the heater probe. All temperature sensors were located in sapwood and captured sap flux of the three trees. Volumetric sap flow was calculated from heat transport velocity and corrected for wounding, sapwood area, volume fraction of wood and water following *Green et al*. [2003] and *Burgess et al*. [2001] for the two methods, respectively. Transpiration was converted from volumetric sap flow by the corresponding projected canopy area.

Stem water potential (ψ_{st}) was measured at 15 min intervals with PSY1 Stem Psychrometers (ICT International Pty Ltd., NSW, Australia), which was developed by *Dixon and Tyree* [1984] and has become commercially available in the last a few years. PSY1 measures the temperature of sapwood surface and chamber air, and stem water potential is corrected with the temperature gradient [*Dixon and Tyree*, 1984]. Recently, PSY1 has been applied in studies on different species, such as Drooping Sheoak [*Yang et al*., 2013], two mangrove species [*Vandegehuchte et al*., 2014b], and two betula species [*Patankar et al*., 2013]. Predawn stem water potential (ψ_{pd}) was taken from the average of ψ_{st} between 3:00 A.M. and 5:00 A.M., with the assumption that water potentials in the tree and root-zone soil have reached an equilibration at this time after water redistribution in the plant-soil system.

2.3. Canopy Conductance Model Construction

The main objective of this study is to select a proper canopy conductance model for a specific environment. Although a two-leaf model that calculates water, carbon, and energy fluxes for both sunlit and shaded leaves [*Wang and Leuning*, 1998] is considered better than the big-leaf model [*Dai et al.,* 2004], the latter is still the most commonly used one for transpiration estimate in land surface models. Therefore, we follow previous studies such as *Lu et al*. [2003] to calculate canopy conductance from the inversion of Penman-Monteith equation:

$$g_c = \frac{g_a \gamma \lambda k_e E_c \rho_w}{\Delta A_c + k_t \rho_a C_p D g_a - \lambda(\Delta+\gamma) k_e E_c \rho_w} \tag{1}$$

where g_c is canopy conductance [m/s]; g_a is aerodynamic conductance [m/s]; γ is psychrometric constant [kPa/°C]; λ is latent heat of vaporization [MJ/kg]; E_c is the tree transpiration calculated from sap flow measurements; Δ is the slope of saturation vapor pressure-temperature curve [kPa/°C]; A_c is the available energy allocated to canopy [MJ/(m^{2}h)]; C_p is specific heat of air at constant pressure [MJ/(kg°C)]; D is vapor pressure deficit [kPa]; ρ_a and ρ_w are the density for air and water, respectively [kg/m^3]; and k_t is for units conversion. When E_c is in mm/h, $k_t = 3600$ s/h; when E_c is in mm/d, $k_t = 86{,}400$ s/d. $k_e = 0.001$ is used to convert E_c from mm/d (mm/h) to m/d (m/h), so that the unit of g_c is m/s.

The available energy was partitioned for canopy (A_c) and substrate according to Beer's law following *Shuttleworth and Wallace* [1985]:

$$A_c = (R_n - G)(1 - e^{-\kappa \cdot LAI}) \tag{2}$$

R_n is net radiation, G is ground heat flux, both in W/m^2; LAI is leaf area index; κ is extinction coefficient, prescribed as 0.7 following [*Yang et al*., 2013]. Other variables in equation (1) are calculated according to FAO irrigation and drainage paper 56 [*Allen et al*., 1998].

We consider four factors that influence the canopy conductance, which are air temperature (T), vapor pressure deficit (D), solar radiation (R_s), and predawn stem water potential (ψ_{pd}). Canopy conductance is modeled following Jarvis-Stewart approach [*Jarvis*, 1976; *Stewart*, 1988].

$$g_c = g_{\max} LAI \cdot f(D) f(T) f(R_s) f(\psi_{pd}) \tag{3}$$

where g_{max} represents the stomata conductance of unstressed vegetation under optimal conditions [m/s].

Different formulae coexist in published studies for each stress function in equation (3). For instance, $f(D)$ is linearly expressed in *Aphalo and Jarvis* [1991], while exponentially in *White et al*. [1999]. In this study, we

focus on two commonly used functions for each factor (from Table 1 and studies cited in this section), and combine them in different ways, then the most appropriate model is determined by comparing simulation results.

One of the solar radiation functions is adopted from *Stewart* [1988] in equation (4a), in which R_{sH} is the approximate maximum solar radiation, and given 350 (W/m^2) for daily step calculations according to the measurements. Another response function that is widely used in land surface models is given in equation (4b) [*Chen and Dudhia*, 2001]. In both equations, k_{Rs} is a fitting parameter [W/m^2].

$$f(R_s)=\frac{R_s}{R_s+k_{Rs}}\frac{R_{sH}+k_{Rs}}{R_{sH}} \tag{4a}$$

$$f(R_s)=\frac{1/(g_{\max}\times 5000)+f}{1+f},\quad f=0.55\frac{R_s}{k_{Rs}}\frac{2}{LAI} \tag{4b}$$

The effect of vapor pressure deficit is expressed exponentially (equation (5a)) in *Whitley et al*. [2009], and linearly (equation (5b)) in other models [*Stewart*, 1988; *Noilhan and Planton*, 1989]. In both equations, k_D is a fitting parameter [kPa^{-1}].

$$f(D)=e^{-k_D D} \tag{5a}$$

$$f(D)=1-k_D D \tag{5b}$$

A second-order polynomial function of air temperature T (in °C) in equation (6a) is originally proposed by *Jarvis* [1976] and used in SiB model [*Sellers et al*., 1986], and extended by *Dickinson* [1984, 1987]. Temperature function in *Jarvis* [1976] is essentially the same with that in *Dickinson* [1984, 1987], and it requires specification of the optimum, upper-limit and lower-limit temperatures. In this study, we choose the temperature function in *Dickinson* [1984]. Equation (6b) is a linear model used in *Stewart* [1988]. T_o is the temperature [°C] at which transpiration rate reaches the maximum. In equations (6a) and (6b), k_T is a fitting parameter.

$$f(T)=1-k_T(T_o-T)^2 \tag{6a}$$

$$f(T)=1-k_T(T_o-T) \tag{6b}$$

For stem water potential, the relationship given in equation (7a) is adopted from *Jarvis* [1976] and that in equation (7b) is from *Choudhury and Idso* [1985] and *Lhomme et al*. [1998]. Root water uptake model described by *Feddes et al*. [1978] gives a relationship between plant water stress and soil water potential: under extremely dry and wet conditions, transpiration rate is assumed to be zero, and in a certain range of soil water potential, transpiration reaches the highest rate; and in other soil moisture conditions transpiration is linearly related to soil water potential. Following this pattern, we propose an upper and a lower limit for stem water potential (ψ_u and ψ_l) at which tree transpires water at the maximum and zero rates respectively; when potential is between ψ_l and ψ_u, $f(\psi_{pd})$ is linearly interpolated. The function is given in equation (7c). Parameter ψ_m (MPa) in equation (7a) is the value of ψ_{pd} at which $f(\psi_{pd})$ extrapolates to 0; ψ_m in equation (7b) gives the water potential limit beyond which the transpiration is strongly limited by water stress [*Lhomme et al*., 1998]. In both equations, k_ψ is a fitting parameter.

$$f(\psi_{pd})=1-e^{-k_\psi(\psi_{pd}-\psi_m)} \tag{7a}$$

$$f(\psi_{pd})=\frac{1}{1+(\psi_{pd}/\psi_m)^{k_\psi}} \tag{7b}$$

$$f(\psi_{pd})=\begin{cases}0, & \psi_{pd}\le\psi_l\\ \dfrac{\psi_{pd}-\psi_l}{\psi_u-\psi_l}, & \psi_l<\psi_{pd}<\psi_u\\ 1, & \psi_{pd}\ge\psi_u\end{cases} \tag{7c}$$

Table 1. Response Functions of Vegetation Conductance to a Series of Factors in the Literature[a]

Site	Species	Response Functions	Source	Notations
Fetteresso Forest, UK & Cedar River Forest, Washington, USA	Sitka spruce & Douglas fir	$f(Q) = k_1k_2(Q - k_3)/[k_1 + k_2(Q - k_3)]$ $f(T) = k_1(T - T_l)(T_h - T)^{k2}$ $f(D) = 1 - k_1D$ $f(\psi_l) = 1\text{-}\exp[-k_1(\psi_l - \psi_m)]$	*Jarvis* [1976]	k_x (x = 1, 2, . . .) is parameter for each equation. Q: photon flux density. T_h, T_l: high and low leaf temperature.
	Golden delicious apple trees	$f(Q) = 1/(1 + k_1/Q)$ $f(D) = 1 - k_2D$	*Thorpe et al.* [1980]; *Warrit et al.* [1980]	ψ_l: leaf water potential. ψ_m: value of ψ_l when $g_s = 0$.
U.S. Water Conservation Laboratory in Phoenix, Arizona	Anza wheat (*Triticum aestivum, L., cv. Anza*)	$f(\psi_l) = [(1 + \psi_l/\psi_{cr})^{k3}]^{-1}$	*Choudhury and Idso* [1985]	ψ_{cr}: critical leaf water potential beyond which transpiration is strongly limited by water stress.
Thetford Forest, Norfolk, England	Scots pine (*Pinus sylvestris (L.)*)	$f1(Rs) = k_1(Rs - 1000) + 1$ $f1(D) = 1 - k_2D$ $f1(T) = k_3(T - 30) + 1$ $f1(\delta\theta) = 1 - k_4\delta\theta$ --- $f2(Rs) = (1000 + k_1)Rs/1000/(k_1 + Rs)$ $f2(D) = 1 - k_2D$ $f2(T) = k_3(T - T_l)(T_h - T)^{k4}$ $f2(\delta\theta) = 1 - \exp[k_4(\delta\theta - \delta\theta_m)]$	*Stewart* [1988]	$\delta\theta$: soil moisture deficit. $\delta\theta_m$: empirically determined maximum value of $\delta\theta$. Rsmin: minimum stomatal resistance. T in Kelvin degree. θ_{cr}: critical point volumetric water content.
Southern Great Plains of the United States	Grass, winter wheat	$f(Rs) = (Rsmin/5000 + f)/(1 + f)$ $f = 0.55Rs/k_1*2/LAI$ $f(D) = 1 - k_2D$ $f(T) = 1 - 0.0016(T - 298)^2$ $f(\theta) = 1$, when $\theta > \theta_{cr}$ $f(\theta) = 0$, when $\theta < \theta_{wp}$ $f(\theta) = (\theta - \theta_{wp})/(\theta_{cr} - \theta_{wp})$, when $\theta_{wp} \le \theta \le \theta_{cr}$	*Alfieri et al.* [2008]	θ_{wp}: wilting point volumetric water content. Q_h: incident radiation at top of canopy. Q_{50}: value of Q, when g_s is half of the maxima. k_Q: light extinction coefficient. ψ_{pd}: predawn leaf water potential.
Frankfort State Forest, eastern Transvaal, South Africa	*Eucalyptus grandis*	$f(Q) = k_1k_2Q/(k_1 + k_2Q)$ $f(D) = k_3\exp(k_4D)$	*Dye and Olbrich* [1993]	
	Eucalyptus grandis and other species (refer to references)	$f(D) = 1/(1 + D/k_1)$ $f(Q) = \ln\{(Q_h + Q_{50})/[Q_h \exp(-k_QLAI) + Q_{50}]\}/k_Q$ $f(Rs) = (1000 + k_1)Rs/[1000(k_1 + Rs)]$ $f(\psi_l) = [(1 + \psi_l/\psi_{cr})^{k3}]^{-1}$ $f(D) = 1 - k_2D$	*Leuning* [1995] *Lohammar et al.* [1980] *Kelliher et al.* [1995] *Leuning et al.* [2008]	
South-east Tasmania	*Eucalyptus globulus* and *Eucalyptus nitens*	$f(Q) = k_1\{k_2Q + 1 - [(k_2Q + 1)^2 - k_3Q]^{0.5}\}$ $f(T) = k_4(T - T_l)(T_h - T)^{k5}$ $f(D) = 1.1\exp(-0.63D)$ $f(\psi_{pd}) = 1.09\exp(-1.27\psi_{pd})$	*White et al.* [1999]	
Liverpool Plains, north-western NSW	*Eucalyptus crebra* and *Callitris glaucophylla*	$f(Rs) = (1000 + k_1)Rs/[1000(k_1 + Rs)]$ $f(D) = \exp(-k_3D)$ $f(\theta) = 1$, when $\theta > \theta_{cr}$ $f(\theta) = 0$, when $\theta < \theta_{wp}$ $f(\theta) = (\theta - \theta_{wp})/(\theta_{cr} - \theta_{wp})$, when $\theta_{wp} \le \theta \le \theta_{cr}$	*Whitley et al.* [2009]	

[a]CO_2 concentration is not considered in this study, so functions with regard to carbon are not listed.

2.4. Model Selection and Parameter Optimization

Canopy conductance models were examined at daily time step. Measurements on tree 2 in 2012 covered the longest period including both dry and wet days (mostly in dry warm season) compared to the other two trees. Data from tree 2 on rainy days were filtered out, the rest were divided into two groups (one contains data in the order of 1, 3, 5, . . . and the other 2, 4, 6, . . ., respectively). The first group was used to train the model, and the second group was used to test the model. Data collected on tree 1 in 2011 and tree 3 in 2014 were also filtered and used for model testing.

Unlike some studies using only two or three response functions (examples in Table 1), we presume that four factors are all functioning significantly in regulating the canopy conductance. Therefore, we first examined 24 combinations of the functions (equations (4a)–(7c)), and then tested the importance of temperature by setting *f*(*T*) to 1 (giving 12 additional models) and comparing the results with those using equations (6a) and (6b). The 36 model constructions are illustrated in Figure 1. Parameters for each g_c model were

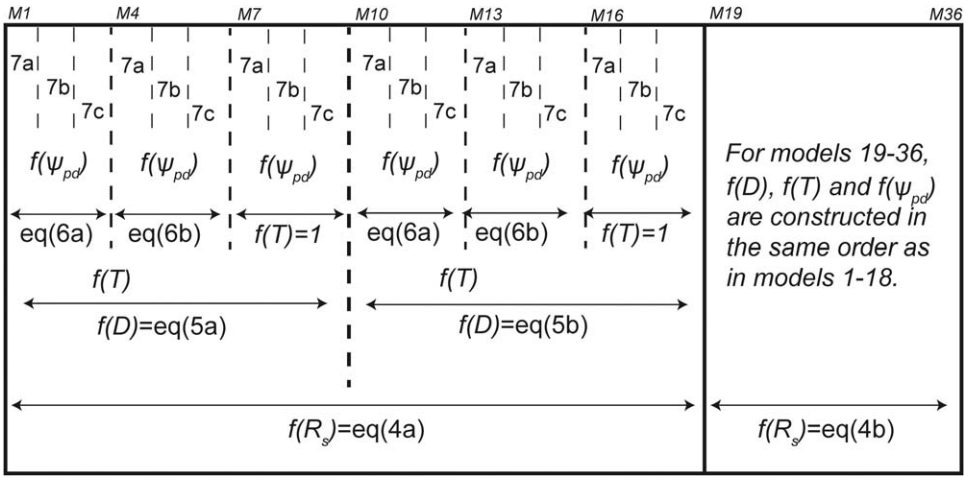

Figure 1. Illustration of 36 canopy conductance models composed of different response functions for D, R_s, T, and ψ_{pd}. Symbols on top indicate the model numbers (*M1-M36*).

obtained using the DiffeRential Evolution Adaptive Metropolis (DREAM) model [*Vrugt et al*., 2009]. DREAM runs multiple different chains simultaneously for global exploration and automatically tunes the scale and orientation of the proposal distribution in randomized subspaces during the search. More details about the model can be found in *Vrugt et al*. [2009]. The DREAM is performed for each conductance model by 20,000 iterations, in order to make it highly possible that the final results are at their global optimum.

3. Results and Discussion

3.1. Microclimate, Sap Flow, and Stem Water Potential

Part of the measurement results for tree 2 is demonstrated in Figure 2 at half-hourly intervals. Daily data of sap flow, stem water potential, and microclimate were calculated from the original 30 and 15 min measurements. Daily mean temperature in the measurement periods of 2011, 2012, and 2014 was 17, 20, and 15°C,

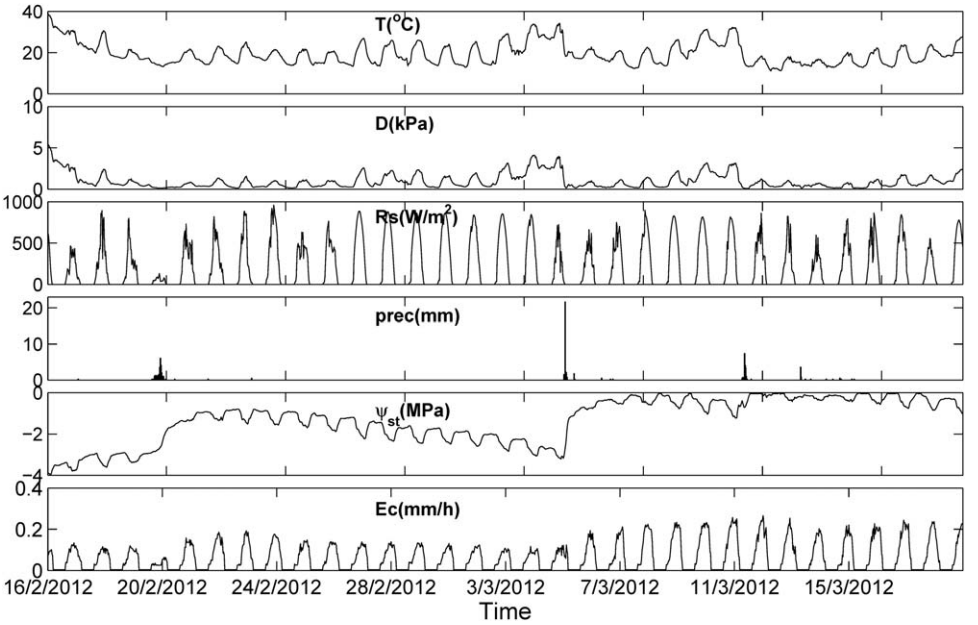

Figure 2. Part of microclimatic variables, tree water use, and stem water potential data for tree 2 in 2012 at 30 min intervals. T is air temperature, D is vapor pressure deficit, R_s is solar radiation, *prec* is rainfall, ψ_{st} is stem water potential, and E_c is transpiration.

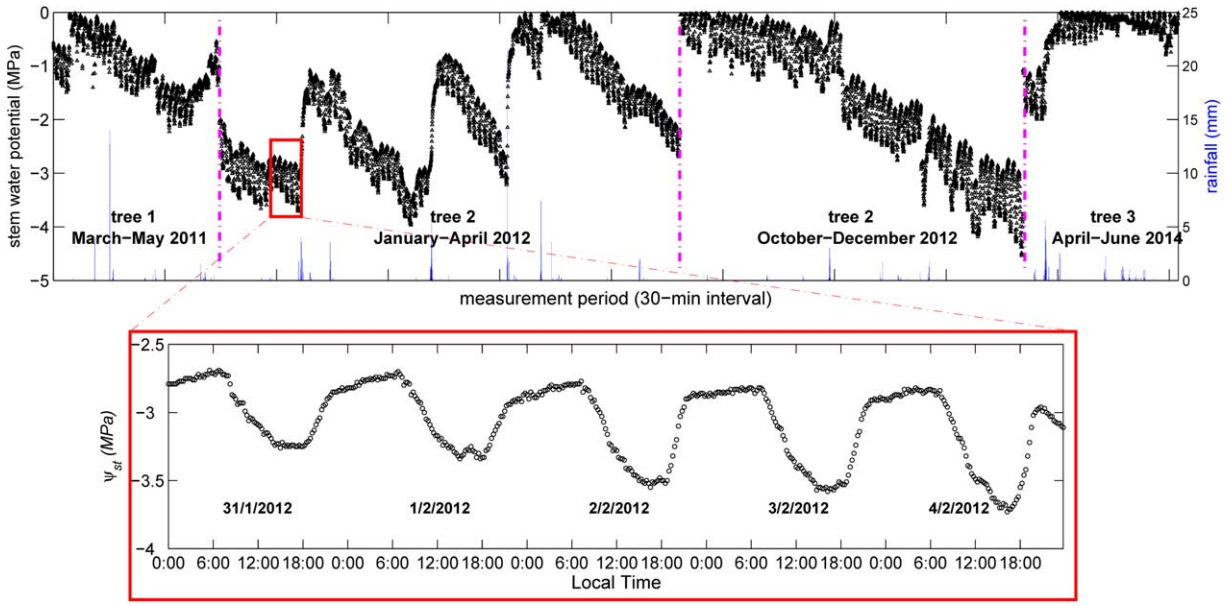

Figure 3. Part of rainfall and stem water potential measurements (30 min intervals) for three trees. Bottom plot gives stem water potential data of tree 2 at 15 min intervals for the part of data enclosed in red rectangle in the top plot. Pink dash lines (top plot) separate the three measurement periods.

respectively. Most days in the measurement period for tree 3 were cloudy or rainy, which affected the data quality in this period.

Figure 2 shows that the changes of air temperature (T) and vapor pressure deficit (D) with time are similar. Stem water potential (ψ_{st}) responds to rainfall sensitively in dry periods. After rainfall occurs, ψ_{st} increases quickly to a high value within a short time range such as a few hours, which depends on the rainfall amount and duration. The relationship among stem water potential, solar radiation, and tree water use indicates that tree water use is mainly constrained by water availability rather than energy in summer. Particularly, daily stem water potential decreased continuously from October to December of 2012 (Figure 3), when soil became drier. Transpiration rate also decreased during this period. Stem water potential data indicate that Sheoak recovers xylem water storage in nighttime and likely has reached an equilibrium state before predawn (Figures 2 and 3). The daily average difference between the maximum stem water potential (around predawn) and minimum stem water potential (late afternoon 15:00–16:00) was around 1 MPa for clear days in dry season (Figure 3).

Relationship between canopy conductance and the four influencing factors (T, D, R_s, and ψ_{pd}) is given in Figure 4 for three trees in different measurement periods. The calculated canopy conductance was larger in spring and autumn than in summer. The maximum canopy conductance was observed in early October 2012 after the rainy season, about 0.015 m/s.

3.2. Model Optimization and Comparison

To compare the conductance models and determine the most appropriate one, we calculated correlation coefficient (r), root-mean-square error ($RMSE$), and slope of linear regression (with zero intercept) between simulated and calculated g_c from equation (1) for each model based on the training and testing data sets. Results are given in Figure 5. We notice that the results of model testing based on data set of 2012, reflected in correlation coefficients, $RMSE$, and slopes, appear better than those from model calibration based on the training data set of 2012, which is against our intuition. A careful check suggests that this is because some extreme large conductance values were accidentally allocated to the training data set. The calibrated models with training data from tree 2 in 2012 were also applied for tree 1 in 2011 and tree 3 in 2014 for testing. Results showed consistent overestimation of canopy conductance for these two trees (fitting slopes larger than 1, Figure 5c). In this exercise, we assumed a constant g_{max} which was obtained from training data of tree 2 collected in spring, summer, and early autumn, while the data of tree 1 and tree 3 were collected in midautumn and late autumn. In fact, as pointed out by *Schulze et al*. [1994], *Ronda et al*. [2001], and *Alfieri*

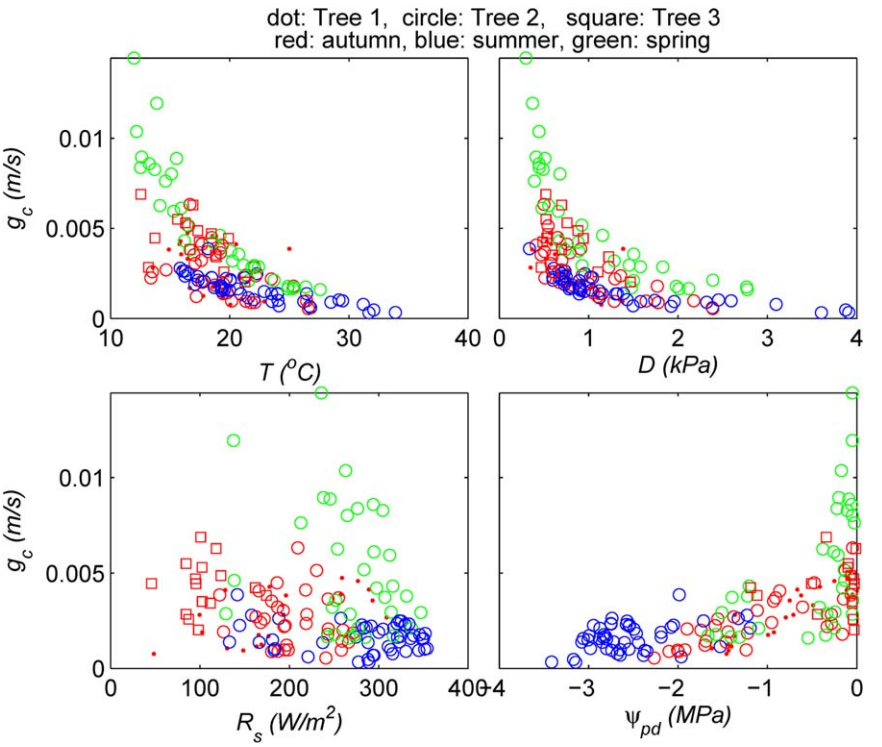

Figure 4. Relationship between canopy conductance and four influencing factors (T, D, R_s, and ψ_{pd}). Data include all measurements (excluding rainy days) for three trees in 2011, 2012, and 2014.

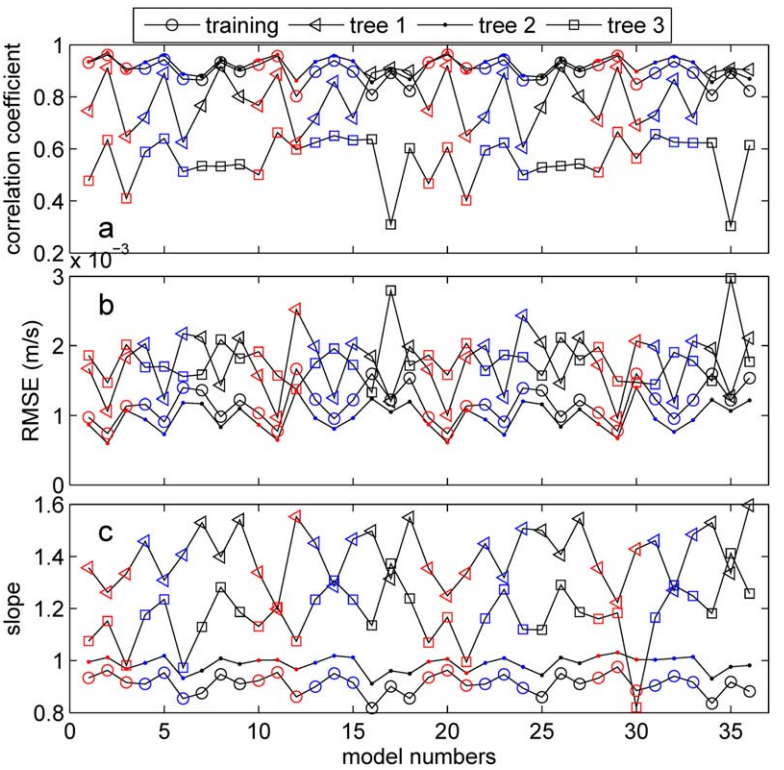

Figure 5. Comparison of model performance using training data in 2012 and testing data in 2011 (tree 1), 2012 (tree 2), and 2014 (tree 3). Slope in plot *c* is from linear regression between simulated and PM-calculated g_c with zero intercept. Red color highlights models using equation (6a), blue stands for models using equation (6b), and black symbolizes models without temperature function. Refer to Figure 1 for model numbers and the relevant response functions.

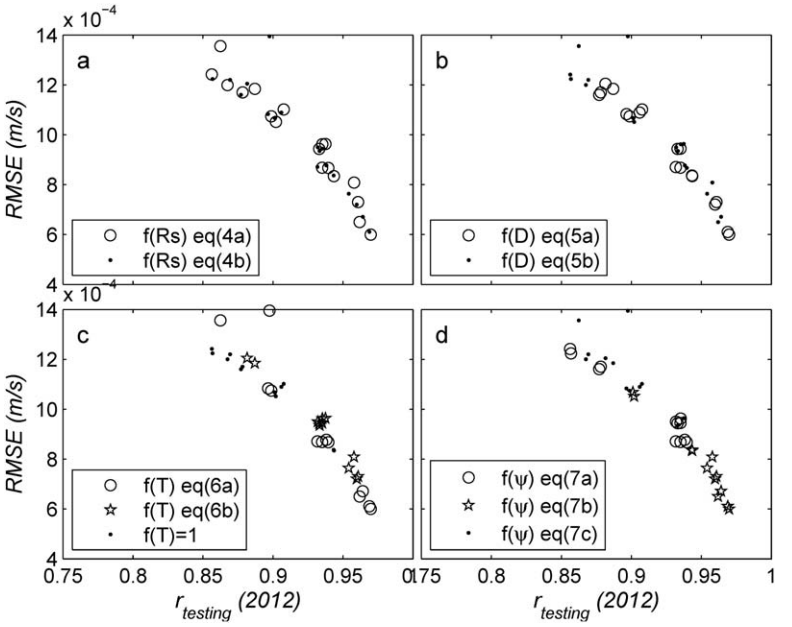

Figure 6. Significance tests of response functions for each influencing factor using *RMSE* and correlation coefficient based on data from tree 2 in 2012. (a) Simulations using equation (4a) for $f(R_s)$ combined with other functions in comparison to simulations using equation (4b) for $f(R_s)$ with other functions. It is the same for (b) $f(D)$, (c) $f(T)$, and (d) $f(\psi_{pd})$. The four figures share the same axes tick labels.

et al. [2008], g_{max} is both time and site specific. Seasonal variability of g_{max} likely interprets the consistent model overestimation for tree 1 in 2011 and tree 3 in 2014. Based on this result, sheoak trees likely have a lower g_{max} in autumn than that in spring and summer.

Figures 5 and 6 show the influence of stress function selection on model performance, and hence suggest the appropriate functions that better fit the calculated canopy conductance. When equations for T, D, and R_s are the same, models using equation (7b) for predawn stem water potential (the middle one of each group of three models in the queue, Figure 5) give better results than models using equations (7a) and (7c). For example, in models 1–3, the correlation coefficient of the training data is 0.94, 0.97, and 0.90, and the root-mean-square error is 0.0009, 0.0006, and 0.0011 m/s. This is particularly clear in Figure 6d, where the results from equation (7b) (pentagrams) appear to be better than those from equations (7a) and (7c) (circles and dots) in terms of both $r_{testing}$ and *RMSE*. When equations for D, R_s, and ψ_{pd} are the same, models with a temperature function fit calculated g_c better than those without a temperature function. For example, in Figure 5, models 2 and 5 give higher correlation coefficients and lower *RMSE* than model 8, and Figure 6c shows that results from equation (6a) (circles) are better than those from equation (6b) (pentagrams); results from models without temperature function (dots) appear to be the worst. Therefore, temperature plays a significant role in canopy conductance modeling and should not be neglected. Figure 6b shows that models using equation (5a) for vapor pressure deficit generate better results than those using equation (5b). Models using the two solar radiation functions give similar results, which implies that it does not matter much which of the two response functions, i.e., equations (4a) and (4b) symbolized by circles and dots in Figure 6a, is used in canopy conductance models.

From statistical results in Figures 5 and 6, model 2 is considered the most suitable model in this study and given in equation (8). This model comprises equation (4a) for solar radiation, equation (5a) for vapor pressure deficit, equation (6a) for temperature, and equation (7b) for predawn stem water potential.

$$g_c = 0.0076 \cdot LAI \cdot \left(\frac{R_s}{R_s+4.6} \cdot \frac{350+4.6}{350}\right) \cdot \left\{e^{-0.75D} \cdot \left[1+0.0128(20-T)^2\right]\right\} \cdot \frac{1}{1+\left(\frac{\psi_{pd}}{-0.87}\right)^{0.74}} \quad (8)$$

Comparison between the calculated g_c from equation (1) and simulated g_c from model 2 for three trees is given in Figure 7. The maximum stomatal conductance g_{max} for this model is 0.0076 m/s; the equivalent

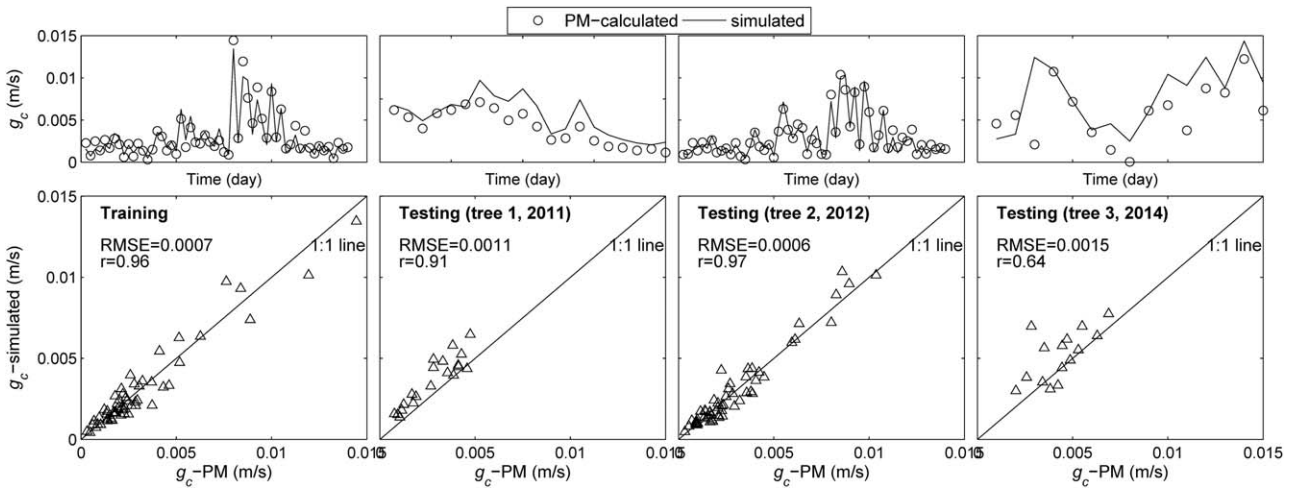

Figure 7. Comparison of canopy conductance calculated from equation (1) and simulated from the best model (model 2). Training data are from tree 2 in 2012, testing data are from tree 1 in 2011, tree 3 in 2014, and the other half of data from tree 2 in 2012.

minimum stomatal resistance for the Droop Sheoak trees is 132 s/m. This number is close to that used in Noah land surface model, which is one of the land surface models used in the Weather Research and Forecasting model [*Hong et al*., 2009], the North American Land Data Assimilation System [*Mitchell et al*., 2004], and the High-Resolution Land Data Assimilation System [*Chen et al*., 2007]. In Noah, the minimum stomatal resistance for needle-leaf evergreen trees is 150 s/m [*Chen and Dudhia*, 2001; *Kumar et al*., 2011]. Transpiration in this study is converted from volumetric sap flow by the projected canopy area. This area may underestimate the effective coverage of the tree for transpiration calculation, thus underestimate the canopy resistance. Nevertheless, this uncertainty of transpiration estimation does not change the model selection results.

3.3. Parameter Values

Relationship between parameters and correlation coefficient for the testing data set ($r_{testing}$) from tree 2 in 2012 is examined and shown in Figure 8, so as to have a better view of the ranges of parameter values for each response function. Testing data in 2011 and 2014 are not plotted in the figure due to the overestimation of conductance for tree 1, and poor data quality for tree 3. Different response functions for each factor show different ranges of parameter values, indicated by the different symbols in the figure. The following discussion on parameter value range is based on models that give correlation coefficient greater than 0.96, and *RMSE* smaller than 0.0008 m/s. For those models, g_{max} ranges from about 0.005 to 0.008 m/s (Figure 8a). k_D range from 0.66 to 0.77 kPa^{-1} for equation (5a), and from 0.24 to 0.32 kPa^{-1} for equation (5b) (Figure 8c). k_T values are negative and do not vary much for equation (6a) but has large variability for equation (6b) (Figure 8d). k_ψ ranges from 0.50 to 0.78, and ψ_m ranges from −0.87 to −0.34 MPa for equation (7b), while k_ψ and ψ_m ranges from 0.39 to 0.17 and from −4.01 to −3.46 MPa for equation (7a) (Figures 8e and 8f). Correlation coefficient is always smaller than 0.95 when using equation (7a) for predawn stem water potential. The values of k_{Rs} ranges from 0 to 10 W/m^2 for both equations (4a) and (4b) (Figure 8b). The values of k_D for equation (5b) is less variable than that for equation (5a). The parameter values discussed above were derived based on daily data.

The simulation results of k_T for equation (6a) are negative for all models that use this temperature function (Figure 8d), for example, the one in equation (8) is −0.0128. This results in $f(T)$ greater than 1, which is not compatible with the principle of equation (3) that $f(T)$, $f(R_s)$, $f(D)$, and $f(\psi_{pd})$ should lie between 0 and 1 [*Stewart*, 1988]. Figure 4 shows that the relationship between g_c and T is similar to g_c and D. This relationship is different from the ones illustrated in other studies such as *Jarvis* [1976] and *White et al*. [1999] in which the relationship fits the "downward" parabolic curve, as is also shown in *Noilhan* and *Planton* [1989] and *Chen et al*. [1996] with $k_T = 0.0016$ for the same equation. The important assumption of analyzing the relationship between canopy conductance and influencing factors is that the factors should be independent of each

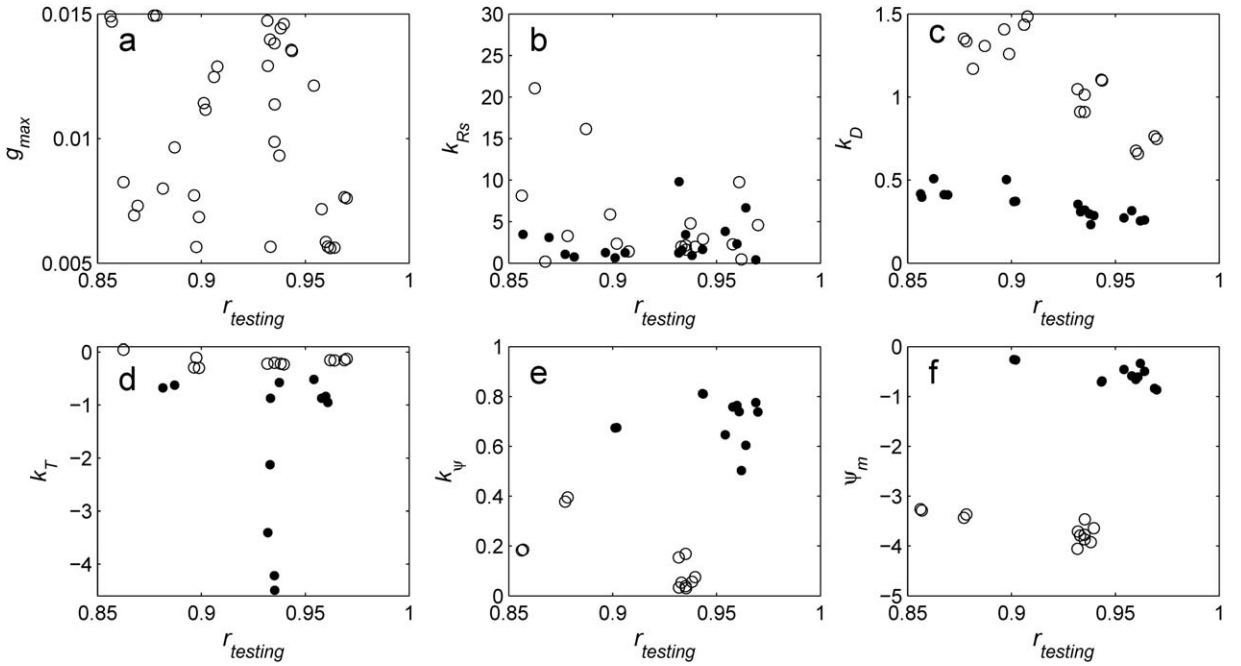

Figure 8. Parameter (g_{max}, k_{Rs}, k_D, k_T, k_ψ, and ψ_m) value ranges for different response functions. (a) Results from all simulations; (b) circles symbolize results from models using equation (4a), and dots equation (4b); (c) circles symbolize results from models using equation (5a), and dots equation (5b); (d) circles symbolize results from models using equation (6a), and dots equation (6b); (e and f) Circles symbolize results from models using equation (7a), and dots equation (7b). k_T in plot (d) is multiplied by 10 for a better view.

other [*Macfarlane et al.*, 2004]. However, it is difficult to distinguish the effects of *T* and *D* on canopy conductance, because *T* and *D* are usually highly correlated [*Alves and Pereira*, 2000]. This correlation is especially strong in this study, showing a linear correlation coefficient of 0.92, which explains the similar relationship between g_c-*T* and g_c-*D* (Figure 4). To examine if the negative k_T only applies to tree 2 in 2012 or it also applies to other sheoak trees in other years, we ran the DREAM optimization with data from tree 1 in 2011 and tree 3 in 2014. Results also gave negative k_T values.

The measurements and optimization results suggest that effects of air temperature on canopy conductance are not appropriately expressed by *f*(*T*) in this study. We further examined the relationship between functions of temperature and vapor pressure deficit in model 2 (Figure 9) using all data from tree 2 in 2012, by comparing *f*(*T*), *f*(*D*), and *f*(*DT*) which is the product of *f*(*T*) and *f*(*D*). The results show that when *T* is between 18 and 22°C, *f*(*DT*) is almost the same as *f*(*D*), which implies that the influence of temperature on canopy

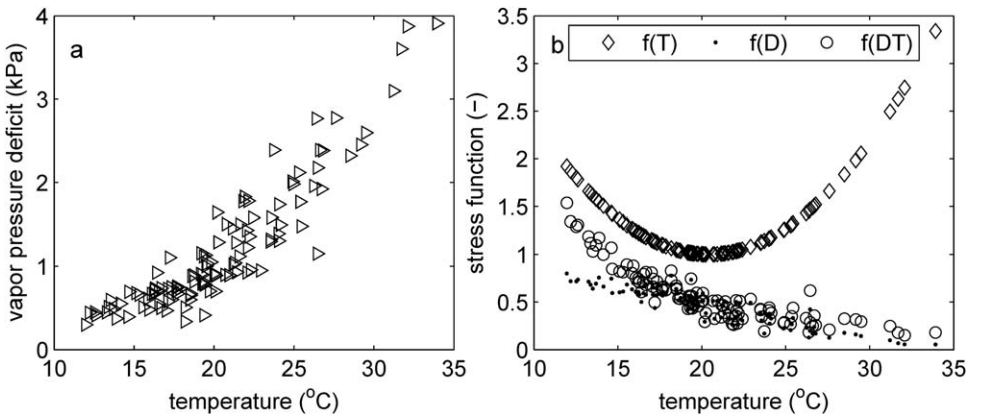

Figure 9. (a) Relationship between temperature and vapor pressure deficit and (b) the response functions *f*(*T*), *f*(*D*), and *f*(*DT*) [=*f*(*T*) × *f*(*D*)] of model 2.

conductance is very small in this temperature range. However, when T is below 18°C, $f(DT)$ is apparently larger than $f(D)$ but smaller than $f(T)$; when T is above 22°C, $f(DT)$ is also larger than $f(D)$, but to a small degree. Mostly, the values of $f(DT)$ lies between 0 and 1, consistent with the principle of a stress function [*Stewart*, 1988]. Therefore, we suggest that the effect of vapor pressure deficit and air temperature should be combined into one, such as $f(DT)$.

4. Conclusions

Stomata regulation of water transport in the soil-plant-atmosphere continuum is vegetation and climate specific. Different models are used to quantify this regulation to help understand climate control on tree water use by relating stomata conductance to environment conditions. Different response functions are presented in literature for conductance modeling for different species and climate conditions. We constructed canopy conductance models by combining the commonly used functions in different ways and selected the best one for our study species and climate. The method in this study shows a success in selecting the suitable canopy conductance model. This optimization method should also be applicable in other environment, even with different response functions, provided that enough data are collected for the targeted influencing factors.

Selection of response functions is very important for canopy conductance modeling. For Drooping Sheoak in this study, models that better simulate canopy conductance comprise a parabolic function of air temperature, an exponential function of vapor pressure deficit and a hyperbolic function of predawn stem water potential. Selection of either of the solar radiation functions does not make significant difference in the model performance. Canopy conductance models that take temperature functions into account resulted in better simulations than those without a temperature function. Therefore, temperature effect should not be neglected in canopy conductance model. The resulted temperature stress function gives values greater than 1, which is considered to be associated with highly interdependence of air temperature and vapor pressure deficit. Combined stress function of air temperature and vapor pressure deficit suggests a sound physical meaning with the values between zero and unity.

Acknowledgments
This project is supported by National Centre for Groundwater Research and Training (NCGRT, Australia). The first author is supported by China Scholarship Council and *NCGRT* for his PhD study at Flinders University of South Australia. Xiang Xu and Yunhui Guo provided assistance in the field. Constructive comments and suggestion from three anonymous reviewers significantly improve the manuscript.

References

Alfieri, J. G., D. Niyogi, P. D. Blanken, F. Chen, M. A. LeMone, K. E. Mitchell, M. B. Ek, and A. Kumar (2008), Estimation of the minimum canopy resistance for croplands and grasslands using data from the 2002 International H_2O Project, *Mon. Weather Rev.*, *136*(11), 4452–4469.

Allen, R. G., L. S. Pereira, D. Raes, and M. Smith (1998), *Crop evapotranspiration: Guidelines for computing crop water requirements, FAO Irrig. and Drain. Pap. 56*, Rome.

Alves, I., and L. S. Pereira (2000), Modelling surface resistance from climatic variables?, *Agric. Water Manage.*, *42*(3), 371–385.

Aphalo, P. J., and P. G. Jarvis (1991), Do stomata respond to relative humidity?, *Plant Cell Environ.*, *14*(1), 127–132.

Avissar, R., and R. A. Pielke (1989), A parameterization of heterogeneous land surfaces for atmospheric numerical-models and its impact on regional meteorology, *Mon. Weather Rev.*, *117*(10), 2113–2136.

Ball, J. H., L. E. Woodrow, and J. A. Beny (1987), A model predicting stomatal conductance and its contribution to the control of photosynthesis under different environmental conditions, paper presented at Progress in Photosynthesis Research, Martinus Nijhoff, Providence.

Burgess, S. S. O., M. A. Adams, N. C. Turner, C. R. Beverly, C. K. Ong, A. A. H. Khan, and T. M. Bleby (2001), An improved heat pulse method to measure low and reverse rates of sap flow in woody plants, *Tree Physiol.*, *21*(9), 589–598.

Chapman, T. F., and D. C. Paton (2007), Casuarina ecology: Factors limiting cone production in the drooping sheoak, Allocasuarina verticillata, *Aust. J. Bot.*, *55*(2), 171–177.

Chen, F., and J. Dudhia (2001), Coupling an advanced land surface-hydrology model with the Penn State-NCAR MM5 modeling system. Part I: Model implementation and sensitivity, *Mon. Weather Rev.*, *129*(4), 569–585.

Chen, F., K. Mitchell, J. Schaake, Y. K. Xue, H. L. Pan, V. Koren, Q. Y. Duan, M. Ek, and A. Betts (1996), Modeling of land surface evaporation by four schemes and comparison with FIFE observations, *J. Geophys. Res.*, *101*(D3), 7251–7268.

Chen, F., et al. (2007), Description and evaluation of the characteristics of the NCAR high-resolution land data assimilation system, *J. Appl. Meteorol. Climatol.*, *46*(6), 694–713.

Choné, X., C. Van Leeuwen, D. Dubourdieu, J. P. Gaudillère (2001), Stem water potential is a sensitive indicator of grapevine water status, *Ann. Bot.*, *87*(4), 477–483.

Choudhury, B. J., and S. B. Idso (1985), An empirical-model for stomatal-resistance of field-grown wheat, *Agric. For. Meteorol.*, *36*(1), 65–82.

Collatz, G. J., J. T. Ball, C. Grivet, and J. A. Berry (1991), Physiological and environmental regulation of stomatal conductance, photosynthesis and transpiration: A model that includes a laminar boundary layer, *Agric For. Meteorol.*, *54*(2–4), 107–136.

Comstock, J., and M. Mencuccini (1998), Control of stomatal conductance by leaf water potential in *Hymenoclea salsola* (T & G), a desert subshrub, *Plant Cell Environ.*, *21*(10), 1029–1038.

Dai, Y. J., R. E. Dickinson, and Y. P. Wang (2004), A two-big-leaf model for canopy temperature, photosynthesis, and stomatal conductance, *J. Clim.*, *17*(12), 2281–2299.

Damour, G., T. Simonneau, H. Cochard, and L. Urban (2010), An overview of models of stomatal conductance at the leaf level, *Plant Cell Environ.*, *33*(9), 1419–1438.

Dickinson, R. E. (1984), Modeling evapotranspiration for three-dimensional global climate models, in *Climate Processes and Climate Sensitivity*, edited by J. E. Hansen and K. Takahashi, *Geophysical Monograph 29*, pp. 58–72, Amer. Geophys. Union, Washington, D. C.

Dickinson, R. E. (1987), Evapotranspiration in global climate models, *Adv. Space Res.*, *7*(11), 17–26.

Dixon, M. A., and M. T. Tyree (1984), A new stem hygrometer, corrected for temperature-gradients and calibrated against the pressure bomb, *Plant Cell Environ.*, *7*(9), 693–697.

Dye, P. J., and B. W. Olbrich (1993), Estimating transpiration from 6-year-old eucalyptus-grandis trees—Development of a canopy conductance model and comparison with independent sap flux measurements, *Plant Cell Environ.*, *16*(1), 45–53.

Eamus, D., and R. Froend (2006), Groundwater-dependent ecosystems: The where, what and why of GDEs, *Aust. J. Bot.*, *54*(2), 91–96.

Edwards, W. R. N., and P. G. Jarvis (1982), Relations between water-content, potential and permeability in stems of conifers, *Plant Cell Environ.*, *5*(4), 271–277.

Feddes, R. A., P. J. Kowalik, and H. Zaradny (1978), *Simulation of Field Water Use and Crop Yield*, Cent. for Agric. Publ. and Doc., Wageningen, Netherlands.

Gash, J. H. C., W. J. Shuttleworth, C. R. Lloyd, J. C. Andre, J. P. Goutorbe, and J. Gelpe (1989), Micrometeorological measurements in Les Landes forest during HAPEX-MOBILHY, *Agric. For. Meteorol.*, *46*(1–2), 131–147.

Green, S., and B. E. Clothier (1988), Water-use of kiwifruit vines and apple-trees by the heat-pulse technique, *J. Exp. Bot.*, *39*(198), 115–123.

Green, S., B. Clothier, and B. Jardine (2003), Theory and practical application of heat pulse to measure sap flow, *Agron. J.*, *95*(6), 1371–1379.

Guan, H. D., X. P. Zhang, G. Skrzypek, Z. Sun, and X. Xu (2013), Deuterium excess variations of rainfall events in a coastal area of South Australia and its relationship with synoptic weather systems and atmospheric moisture sources, *J. Geophys. Res. Atmos.*, *118*, 1123–1138, doi:10.1002/jgrd.50137.

Hong, S. B., V. Lakshmi, E. E. Small, F. Chen, M. Tewari, and K. W. Manning (2009), Effects of vegetation and soil moisture on the simulated land surface processes from the coupled WRF/Noah model, *J. Geophys. Res.*, *114*, D18118, doi:10.1029/2008JD011249.

Jarvis, P. G. (1976), The interpretation of the variations in leaf water potential and stomatal conductance found in canopies in the field, *Philos. Trans. R. Soc. London B*, *273*(927), 593–610.

Kelliher, F. M., R. Leuning, M. R. Raupach, and E. D. Schulze (1995), Maximum conductances for evaporation from global vegetation types, *Agric. For. Meteorol.*, *73*(1–2), 1–16.

Kumar, A., F. Chen, D. Niyogi, J. G. Alfieri, M. Ek, and K. Mitchell (2011), Evaluation of a photosynthesis-based canopy resistance formulation in the Noah Land-Surface Model, *Boundary Layer Meteorol.*, *138*(2), 263–284.

LeMone, M. A., F. Chen, J. G. Alfieri, M. Tewari, B. Geerts, Q. Miao, R. L. Grossman, and R. L. Coulter (2007), Influence of land cover and soil moisture on the horizontal distribution of sensible and latent heat fluxes in southeast Kansas during IHOP_2002 and CASES-97, *J. Hydrometeorol.*, *8*(1), 68–87.

Leuning, R. (1995), A critical-appraisal of a combined stomatal-photosynthesis model for C-3 plants, *Plant Cell Environ.*, *18*(4), 339–355.

Leuning, R., and I. J. Foster (1990), Estimation of transpiration by single trees—Comparison of a ventilated chamber, leaf energy budgets and a combination equation, *Agric. For. Meteorol.*, *51*(1), 63–86.

Leuning, R., Y. Q. Zhang, A. Rajaud, H. Cleugh, and K. Tu (2008), A simple surface conductance model to estimate regional evaporation using MODIS leaf area index and the Penman-Monteith equation, *Water Resour. Res.*, *44*, W10419, doi:10.1029/2007WR006562.

Lhomme, J. P., E. Elguero, A. Chehbouni, and G. Boulet (1998), Stomatal control of transpiration: Examination of Monteith's formulation of canopy resistance, *Water Resour. Res.*, *34*(9), 2301–2308.

Lohammar, T., S. Larsson, S. Linder, and S. O. Falk (1980), Fast-simulation models of gaseous exchange in Scots pine, in *Structure and Function of Northern Coniferous Forests : An Ecosystem Study*, edited by T. Persson, pp. 505–523, Swed. Nat. Sci. Res. Counc., Stockholm.

Lu, P., I. A. M. Yunusa, R. R. Walker, and W. J. Muller (2003), Regulation of canopy conductance and transpiration and their modelling in irrigated grapevines, *Funct. Plant Biol.*, *30*(6), 689–698.

Macfarlane, C., D. A. White, and M. A. Adams (2004), The apparent feed-forward response to vapour pressure deficit of stomata in droughted, field-grown *Eucalyptus globulus* Labill, *Plant Cell Environ.*, *27*(10), 1268–1280.

Mascart, P., O. Taconet, J. P. Pinty, and M. B. Mehrez (1991), Canopy resistance formulation and its effect in mesoscale models—A Hapex perspective, *Agric. For. Meteorol.*, *54*(2–4), 319–351.

Meinzer, F. C., S. A. James, and G. Goldstein (2004), Dynamics of transpiration, sap flow and use of stored water in tropical forest canopy trees, *Tree Physiol.*, *24*(8), 901–909.

Meinzer, F. C., D. R. Woodruff, J. C. Domec, G. Goldstein, P. I. Campanello, M. G. Gatti, and R. Villalobos-Vega (2008), Coordination of leaf and stem water transport properties in tropical forest trees, *Oecologia*, *156*(1), 31–41.

Misson, L., J. A. Panek, and A. H. Goldstein (2004), A comparison of three approaches to modeling leaf gas exchange in annually drought-stressed ponderosa pine forests, *Tree Physiol.*, *24*(5), 529–541.

Mitchell, K. E., et al. (2004), The multi-institution North American Land Data Assimilation System (NLDAS): Utilizing multiple GCIP products and partners in a continental distributed hydrological modeling system, *J. Geophys. Res.*, *109*, D07S90, doi:10.1029/2003JD003823.

Monteith, J. L. (1981), Evaporation and surface-temperature, *Q. J. Roy. Meteorol. Soc.*, *107*(451), 1–27.

Murray, B., M. Zeppel, G. Hose, and D. Eamus (2003), Groundwater dependent ecosystems in Australia: It's more than just water for rivers, *Ecol. Manage. Restor.*, *4*, 109–113.

Noilhan, J., and S. Planton (1989), A simple parameterization of land surface processes for meteorological models, *Mon. Weather Rev.*, *117*(3), 536–549.

Nortes, P. A., A. Pérez-Pastor, G. Egea, W. Conejero, and R. Domingo (2005), Comparison of changes in stem diameter and water potential values for detecting water stress in young almond trees, *Agric. Water Manage.*, *77*(1–3), 296–307.

Palmer, A. R., S. Fuentes, D. Taylor, C. Macinnis-Ng, M. Zeppel, I. Yunusa, and D. Eamus (2010), Towards a spatial understanding of water use of several land-cover classes: An examination of relationships amongst pre-dawn leaf water potential, vegetation water use, aridity and MODIS LAI, *Ecohydrology*, *3*(1), 1–10.

Patankar, R., W. L. Quinton, and J. L. Baltzer (2013), Permafrost-driven differences in habitat quality determine plant response to gall-inducing mite herbivory, *J. Ecol.*, *101*(4), 1042–1052.

Peeters, P. J., T. Gerschwitz, and R. J. Carpenter (2006), Restoring Sheoak Grassy Woodlands on Lower Eyre Peninsula., Report, Department for Environment and Heritage: Government of South Australia, Adelaide, South Australia.

Phillips, N., R. Oren, and R. Zimmermann (1996), Radial patterns of xylem sap flow in non-, diffuse- and ring-porous tree species, *Plant Cell Environ.*, *19*(8), 983–990.

Rao, P., and S. K. Agarwal (1984), Diurnal-variation in leaf water potential, stomatal conductance, and irradiance of winter crop under different moisture levels, *Biol. Plant.*, *26*(1), 1–4.

Richter, H. (1997), Water relations of plants in the field: Some comments on the measurement of selected parameters, *J. Exp. Bot.*, *48*(306), 1–7.

Ronda, R. J., H. A. R. de Bruin, and A. A. M. Holtslag (2001), Representation of the canopy conductance in modeling the surface energy budget for low vegetation, *J. Appl. Meteorol.*, *40*(8), 1431–1444.

Schulze, E. D., F. M. Kelliher, C. Korner, J. Lloyd, and R. Leuning (1994), Relationships among maximum stomatal conductance, ecosystem surface conductance, carbon assimilation rate, and plant nitrogen nutrition—A global ecology scaling exercise, *Annu. Rev. Ecol. Syst.*, *25*, 629–662.

Sellers, P. J., Y. Mintz, Y. C. Sud, and A. Dalcher (1986), A simple biosphere model (sib) for use within general-circulation models, *J. Atmos. Sci.*, *43*(6), 505–531.

Shuttleworth, W. J., and J. S. Wallace (1985), Evaporation from sparse crops—An energy combination theory, *Q. J. Roy. Meteorol. Soc.*, *111*(469), 839–855.

Stewart, J. B. (1988), Modeling surface conductance of pine forest, *Agric. For. Meteorol.*, *43*(1), 19–35.

Thorpe, M. R., B. Warrit, and J. J. Landsberg (1980), Responses of apple leaf stomata—A model for single leaves and a whole tree, *Plant Cell Environ.*, *3*(1), 23–27.

Tuzet, A., A. Perrier, and R. Leuning (2003), A coupled model of stomatal conductance, photosynthesis and transpiration, *Plant Cell Environ.*, *26*(7), 1097–1116.

Tyree, M. T., and S. D. Yang (1990), Water-storage capacity of thuja, tsuga and acer stems measured by dehydration isotherms—The contribution of capillary water and cavitation, *Planta*, *182*(3), 420–426.

Vandegehuchte, M. W., A. Guyot, M. Hubeau, T. De Swaef, D. A. Lockington, and K. Steppe (2014a), Modelling reveals endogenous osmotic adaptation of storage tissue water potential as an important driver determining different stem diameter variation patterns in the mangrove species *Avicennia marina* and Rhizophora stylosa, *Ann. Bot.*, doi:10.1093/aob/mct311, in press.

Vandegehuchte, M. W., A. Guyot, M. Hubau, S. R. E. De Groote, N. J. F. De Baerdemaeker, M. Hayes, N. Welti, C. E. Lovelock, D. A. Lockington, and K. Steppe (2014b), Long-term versus daily stem diameter variation in co-occurring mangrove species: Environmental versus ecophysiological drivers, *Agric. For. Meteorol.*, *192–193*(0), 51–58.

Vrugt, J. A., C. J. F. ter Braak, C. G. H. Diks, B. A. Robinson, J. M. Hyman, and D. Higdon (2009), Accelerating Markov chain Monte Carlo simulation by differential evolution with self-adaptive randomized subspace sampling, *Int. J. Nonlinear Sci. Numer. Simul.*, *10*(3), 273–290.

Wang, Y. P., and R. Leuning (1998), A two-leaf model for canopy conductance, photosynthesis and partitioning of available energy. I: Model description and comparison with a multi-layered model, *Agric. For. Meteorol.*, *91*(1–2), 89–111.

Warrit, B., J. J. Landsberg, and M. R. Thorpe (1980), Responses of apple leaf stomata to environmental-factors, *Plant Cell Environ.*, *3*(1), 13–22.

White, D., C. L. Beadle, P. J. Sands, D. Worledge, and J. L. Honeysett (1999), Quantifying the effect of cumulative water stress on stomatal conductance of *Eucalyptus globulus* and *Eucalyptus nitens*: A phenomenological approach, *Aust. J. Plant Physiol.*, *26*(1), 17–27.

White, R., et al. (2003), SGS Water Theme: Influence of soil, pasture type and management on water use in grazing systems across the high rainfall zone of southern Australia, *Aust. J. Exp. Agric.*, *43*(7–8), 907–926.

Whitley, R., B. Medlyn, M. Zeppel, C. Macinnis-Ng, and D. Eamus (2009), Comparing the Penman-Monteith equation and a modified Jarvis-Stewart model with an artificial neural network to estimate stand-scale transpiration and canopy conductance, *J. Hydrol.*, *373*(1–2), 256–266.

Whitley, R., M. Zeppel, N. Armstrong, C. Macinnis-Ng, I. Yunusa, and D. Eamus (2008), A modified Jarvis-Stewart model for predicting stand-scale transpiration of an Australian native forest, *Plant Soil*, *305*(1–2), 35–47.

Yang, Y. T., H. D. Guan, J. L. Hutson, H. L. Wang, C. Ewenz, S. H. Shang, and C. T. Simmons (2013), Examination and parameterization of the root water uptake model from stem water potential and sap flow measurements, *Hydrol. Processes*, *27*(20), 2857–2863.